International Immunopharmacology 74 (2019) 105676

Contents lists available at ScienceDirect

International Immunopharmacology

journal homepage: www.elsevier.com/locate/intimp

Anti-inflammatory effects of quercetin in a mouse model of MC903-induced atopic dermatitis

Dian-Dong Hou[a,b], Wei Zhang[a,b], Ya-Li Gao[a], Yu-zhe Sun[a], He-Xiao Wang[a], Rui-Qun Qi[a], Hong-Duo Chen[a], Xing-Hua Gao[a,*]

[a] Department of Dermatology, The First Hospital of China Medical University, Key lab of Dermatology, Ministry of Education and Public Health, Shenyang 110001, China
[b] Liaoning University of Traditional Chinese Medicine, Shenyang 110847, PR China

ARTICLE INFO

Keywords:
Quercetin
Anti-inflammatory
Atopic dermatitis

ABSTRACT

In this study, the anti-inflammatory mechanisms of Quercetin (Que) on atopic dermatitis (AD)-like skin lesions was examined. The left ear of mice was applied with MC903, followed by Que. administration daily on the ear for 8 days. Then macroscopic and histologic examination was performed to detect the severity of skin lesions. In the skin section of AD mice, we observed that Que. could reduce the expression of CCL17, CCL22, IL-4, IL-6, IFN-γ and TNF-α. In vitro, the anti-inflammatory effects of Que. were examined on human keratinocytes (HaCaT cells) treated with IFN-γ/TNF-α. To unveil the lncRNAs' regulatory role on Que-activated anti-inflammatory function, the next-generation high-throughput sequencing was performed in HaCat cells with or without Que. treatment, which profiled the expression of lncRNAs and mRNAs, the results illustrated that lnc-C7orf30–2, a lncRNA expressed differentially, was correlated with IL-6 expression. Silencing of lnc-C7orf30–2 by RiboTM lncRNA Smart Silencer proved its role on IL-6 expression. Therefore, the results here demonstrated that topical administration of Que. plays a beneficial role in controlling AD symptoms, which may serve as potential candidate for AD treatment.

1. Introduction

As a skin disease, atopic dermatitis (AD) is induced eczematous skin lesions, with inflammatory characterization. Its prevalence has reached 30% in children and 3% in adults [1]. It has been described that the skin barrier and immunological properties in the epidermal cells of AD mouse model are changed [2]. The barrier disruption and dysfunction of keratinocyte have been observed in patients with AD [3]. The cytokines imbalance of Th2 to Th1 may exert a critical role in the development of atopic dermatitis, which can alter the immune responses and promote hypersensitivity mediated by IgE [4]. Importantly upon exposure to proinflammatory cytokines, the keratinocytes which accounts for 90% cells in the epidermis [5] can secrete types of chemokines and cytokines, including IL-6, CCL22/MDC and CCL17/TARC [6], which may initiate the inflammatory condition in AD [3].

Topical corticosteroid therapy is the most common and effective treatment for AD [7], however, it can increase the risk of recurrence and adverse effects, including skin atrophy and thinning [8]. Therefore, there has been a rising interest to develop safe and effective agents for AD treatment, ranges from plants, animals to microorganisms [9,10].

Quercetin (Que) belongs to a subclass known as flavonoids that exists abundantly in a variety of fruits and vegetables [11], with anti-inflammatory, anti-cancer and anti-atherosclerotic activities [12,13].

It has been reported that topical application of MC903 can trigger an AD-like syndrome, which characterized by the increase of thymic stromal lymphopoietin (TSLP) in mouse keratinocytes [14]. Here, we used MC903-induced AD mouse models for our study. The results showed that the dermatitis severity, mast cells infiltration and the thickness of epidermis were reduced by Que. The expressions of TNF-α, CCL17, CCL22, IFN-γ, IL-4 and IL-6 can also be down-regulated by Que. in the skin section of AD mice. In vitro study revealed that lnc-C7orf30–2, a differentially expressed lncRNA induced by Que. in the IFN-γ/TNF-α-treated HaCaT cells, was correlated with IL-6.

2. Materials and methods

2.1. Animals

C57BL/6 mice (female, weighing 16–18 g, 6–8 weeks old) were housed in a pathogen-free environment with a 12 h light-dark cycle

Abbreviations: MDC, macrophage-derived chemokine; TARC, thymus and activation-regulated chemokine; TSLP, thymic stromal lymphopoietin

* Corresponding author at: Department of Dermatology, The First Hospital of China Medical University, 155N. Nanjing Street, Shenyang 110001, PR China.
E-mail address: gaobarry@hotmail.com (X.-H. Gao).

https://doi.org/10.1016/j.intimp.2019.105676
Received 9 March 2019; Received in revised form 27 May 2019; Accepted 30 May 2019
Available online 07 June 2019

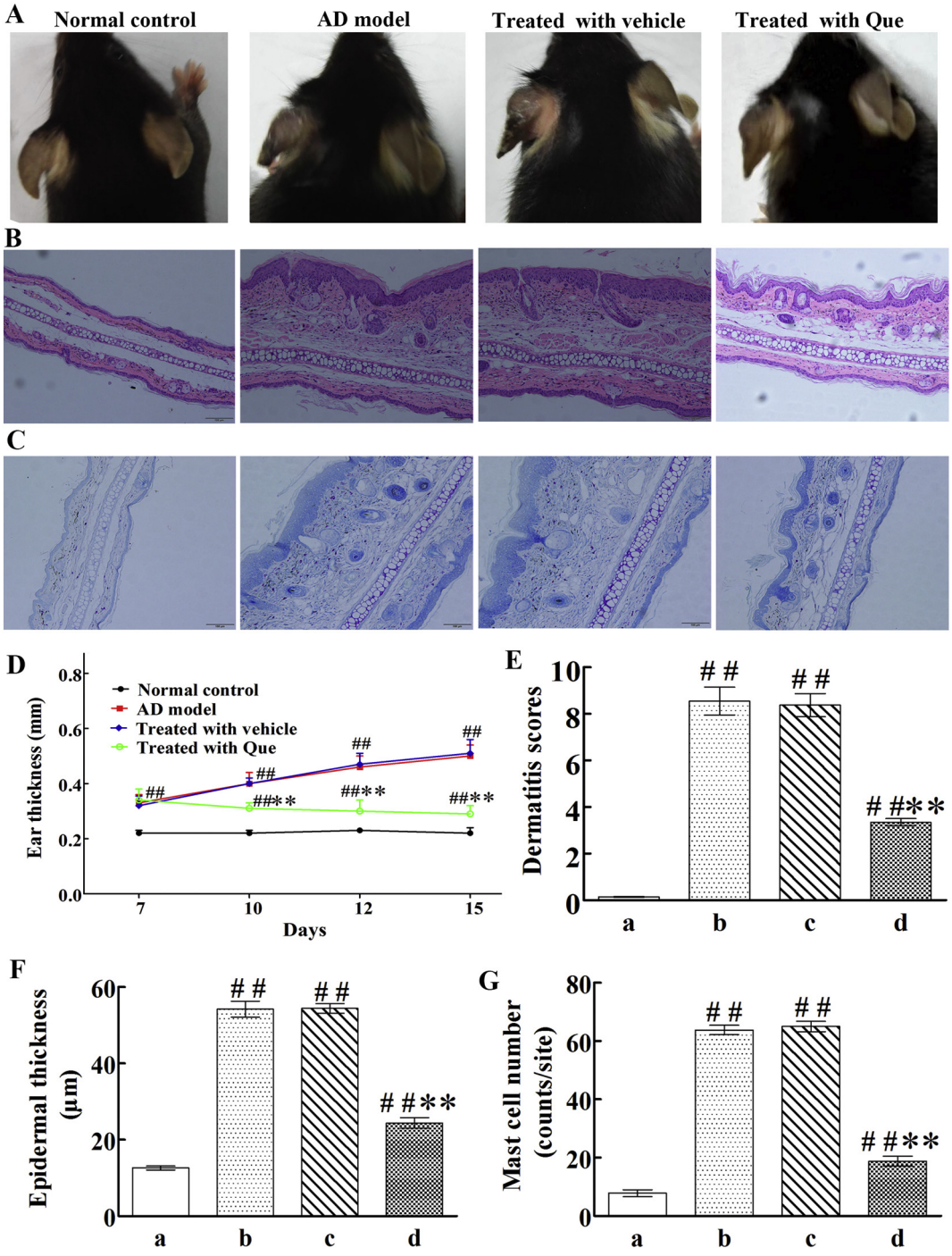

Fig. 1. Effects of Que. on MC903-induced AD-like skin lesions of mice. A. Example of the clinical severity of AD-like skin lesions. B. Ear tissues were stained with H&E, ×200. C. Ear tissues were stained with toluidine blue, ×200. D. Effects of Que. on ear thickness in AD mice. E. The dermatitis scores were defined as the sum of scores based on the various AD symptoms. F. Epidermal thickness was analyzed in H&E-stained tissue. G. The number of mast cells was analyzed in the toluidine blue-stained sections. a. normal control group; b. AD model group; c. treated with vehicle; d. treated with QUE. Data are the means ± SEM ($n = 6$). ## $p < 0.01$ vs. the normal control group; * * $p < 0.01$ vs. the AD model group. (For interpretation of the references to colour in this figure legend, the reader is referred to the web version of this article.)

condition. The mice were fed with a laboratory diet and water. All the mice were purchased from Liaoning Changsheng Biotechnology Co., Ltd. (Benxi, China), and their experiments were approved by China Medical University Ethical Committee (Shenyang, China).

2.2. Que

Que. (CAS# 117-39-5, purity ≥ 98%) was provided by NANJING GOREN BIO-TECHNOLOGY CO., LTD (Nanjing, China). 1% Que. topical cream was prepared by diluting Que. with a basal formulation. The basal formulation included olive oil (10%), cetyl alcohol (3%), tween-80 (4%), glyceryl monostearate (5%), Silicone oil (3%), lanolin (1.5%), glycerin (5%), and water (up to 100.0%). The mixture was heated to 75 °C, the solution was homogenized for 40 min using a magnetic stirrer at 1000 rpm at 75 °C. Que. was also freshly prepared by dissolving in dimethylsulfoxide (DMSO), for in vitro experiment.

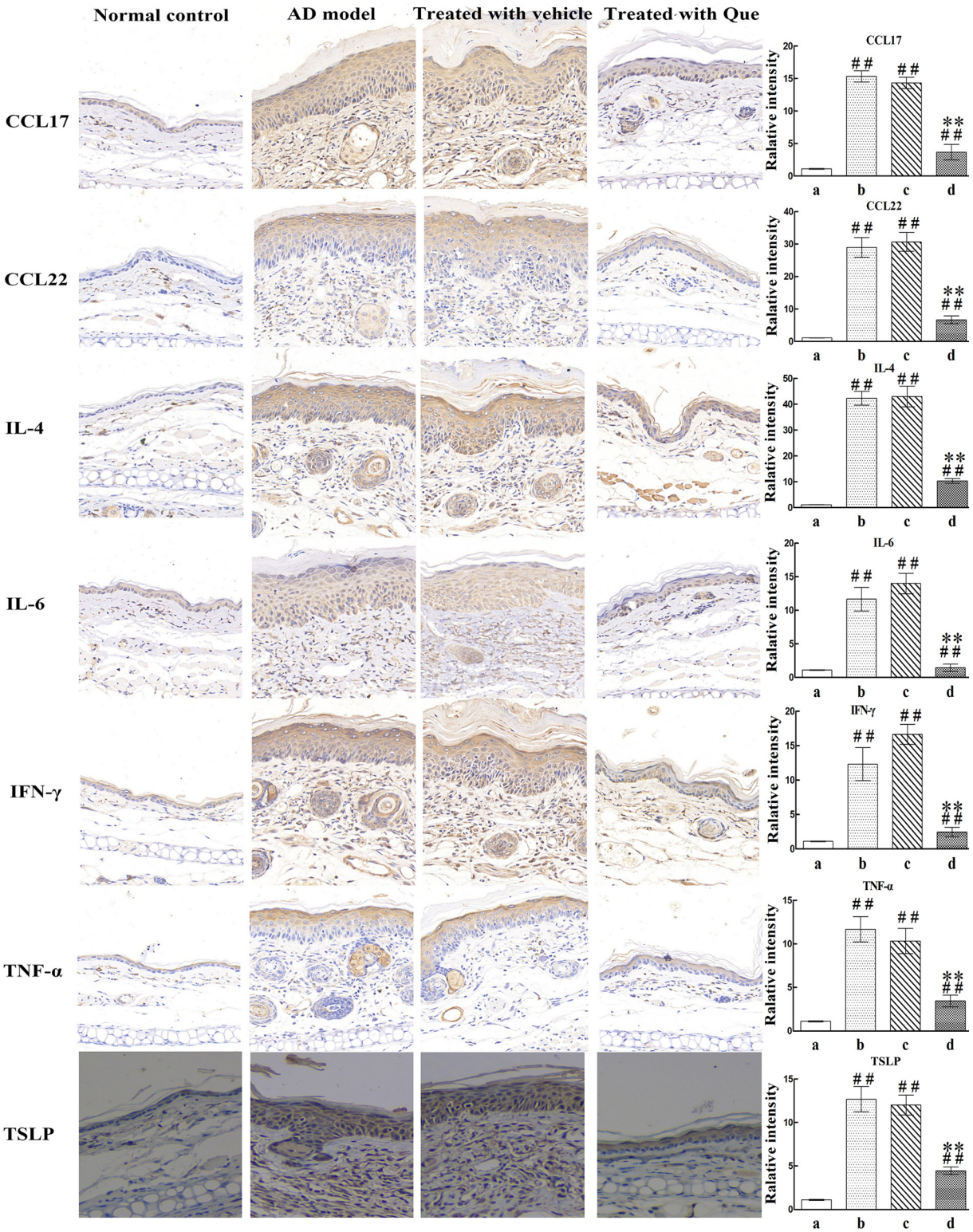

Fig. 2. The effect of Que. on cytokine expressions (CCL17, CCL22, IL-4, IL-6, IFN-γ,TNF-α and TSLP) in ear lesions in MC903-induced AD mice. Cytokine expressions in the sections of ear from mice were detected by immunohistochemistry. Magnification, ×200. The values are shown as mean ± SEM for 6 mice. ## $p < 0.01$ vs. the normal control group; * * $p < 0.01$ vs. the AD model group.

2.3. Atopic dermatitis mouse models and treatment

A total of 24 mice were assigned into 4 groups randomly: normal group, AD model group, vehicle treatment group and Que. treatment group. The MC903 (a low-calcemic analogue calcipotriol of vitamin D3, from Sigma, USA) was applied topically to establish AD mouse model, according to a published protocol [15]. Briefly, 2 nmol MC903 (20 μL, dissolved in ethanol) was topically applied to dorsal side of left ear in AD model group, vehicle treatment group and Que. treatment group once a day for 14 days, while normal control group received 20 μL ethanol on the dorsal side of left ear as solvent control.

AD models were successfully induced by MC903 on 7th day. After

Table 1
Map of antibodies against chemokines on the RayBiotech Human Chemokine Antibody Array G7.

	1	2	3	4	5	6	7	8	9	10	11	12	13	14
A	POS 1	POS 2	POS 3	NEG	NEG	Angiogenin	BDNF	BLC	BMP-4	BMP-6	CKb8–1	CNTF	EGF	CCL11
B	POS 1	POS 2	POS 3	NEG	NEG	Angiogenin	BDNF	BLC	BMP-4	BMP-6	CKb8–1	CNTF	EGF	CCL11
C	CCL24	CCL26	FGF-6	FGF-7	Flt-3 Ligand	CX3CL1	GCP-2	GDNF	CSF2	I-309	IFN-γ	IGFBP-1	IGFBP-2	IGFBP-4
D	CCL24	CCL26	FGF-6	FGF-7	Flt-3 Ligand	CX3CL1	GCP-2	GDNF	CSF2	I-309	IFN-γ	IGFBP-1	IGFBP-2	IGFBP-4
E	IGF-I	IL-10	IL-13	IL-15	IL-16	IL-1α	IL-1β	IL-1ra	IL-2	IL-3	IL-4	IL-5	IL-6	IL-7
F	IGF-I	IL-10	IL-13	IL-15	IL-16	IL-1α	IL-1β	IL-1ra	IL-2	IL-3	IL-4	IL-5	IL-6	IL-7
G	Leptin	LIGHT	MCP-1	MCP-2	MCP-3	MCP-4	M-CSF	MDC	MIG	MIP-1Δ	MIP-3α	NAP-2	NT-3	PARC
H	Leptin	LIGHT	MCP-1	MCP-2	MCP-3	MCP-4	M-CSF	MDC	MIG	MIP-1Δ	MIP-3α	NAP-2	NT-3	PARC
I	PDGF-BB	RANTES	SCF	SDF-1	TARC	TGF-β1	TGF-β 3	TNF-α	TNF-β	NEG	NEG	NEG	NEG	NEG
K	PDGF-BB	RANTES	SCF	SDF-1	TARC	TGF-β1	TGF-β 3	TNF-α	TNF-β	NEG	NEG	NEG	NEG	NEG

that, MC903 was still applied to mice of AD model group, vehicle treatment group and Que. treatment group in the morning. In the afternoon, each group received respective agents for the following 8 days.

2.4. Scoring of dermatitis, ear thickness, and scratching behavior

On the day 7, 10, 12 and 15, the severity of AD, including scoring of dermatitis and ear thickness was measured. Dermatitis severity was scored from 0 to 3, which were named as none, mild, moderate and severe according to the severity of (1) hemorrhage/erythema, (2) itching/crusting, (3) edema, (4) excoriation/erosion [16]. Three investigators performed scoring evaluations throughout the study, then calculate the average. The ear thickness (mm) was evaluated in the same region of the ear using a vernier caliper (Mitutoyo, Kanagawa, Japan).

2.5. Studies of histopathology

The left ear of mice was collected on 15th day of the Que. treatment, followed by fixing with 4% paraformaldehyde. To count the inflammatory cell numbers, H&E staining was performed for the paraffin embeded skin sections (5 μm). Toluidine blue stained sections were used to count mast cells. The number of mast cells was counted in five randomly selected fields of view under a light microscope (magnification, ×200).

2.6. Immunohistochemistry

Tissues embedded in paraffin (5 μm) were placed on frosted microscope slides, followed by incubating in 3% H_2O_2 for 5 min and blocking in normal serum. Then the sections were incubated with IFN-γ, CCL17, CCL22, TNF-α, IL-4 and IL-6 monoclonal antibody (1:100 dilution, Bioss, Beijing, China) at 4 °C for 18 h, followed by incubating with biotinylated IgG. Then the sections were incubated with streptavidin coupled horseradish peroxidase for 15 min (Zhongshan Goldenbridge Biotechnology, Beijing, China), followed by staining with diaminobenzidine (Zhongshan Goldenbridge Biotechnology, Beijing, China) and capturing the pictures for digital quantitative analysis with a digital camera DM6000 (Leica, Germany). Images were collected in three fields at ×200 magnification under the microscope. Image-Pro Plus 6.0 software was used to calculate the ratio of the integral optical density to its area, and the average value was obtained.

2.7. Cell culture

Human keratinocyte HaCaT cells, purchased from ATCC, were cultured in high glucose DMEM (Hyclone) with 10% FBS (Hyclone) in a 5% CO_2 incubator at 37 °C.

2.8. Cytokine antibody arrays

HaCaT at 1.0×10^6 cells/well, cultured in 6-well plates, were treated with Que. (30 or 90 μM) or DMSO for 24 h in 1 mL serum-free media with IFN-γ/TNF-α (10 ng/mL IFN-γ and 10 ng/mL TNF-α, R&D Systems, USA), followed by the supernatants collection, the cytokines were further detected with the RayBiotech Cytokine Antibody Arrays (AAH-CYT-G1000–8). Briefly, blocking buffer was used for treating antibody coated array membranes for 30 min. Then the supernatant (100 μL) was added and incubated overnight at 4 °C. After three wash steps, biotin-conjugated antibodies (70 μL) added to the membranes for 2 h, followed by HRP-coupled streptavidin incubation for 2 h. Detection of spots using chemiluminescence was acquired with semiquantitative analysis of signal intensities from Quantity One software (Bio-Rad Laboratories). Intensities were normalized as a percentage of positive controls on each membrane.

2.9. Enzyme-linked immunosorbent assay

ELISAs kits for IL-6, CCL17, and CCL22 were obtained from CUSABIO (Wuhan, China). Briefly, capture antibody were coated in the 96-well plates, followed by 100 μL supernatants from samples and standards, then incubated with biotinylated antibody (100 μL) for 1 h and subsequently replacing with streptavidin solution (100 μL). After washing steps, 100 μL substrate reagent was added for 30 min, followed by incubating with stop solution (50 μL). optical density at 450 nm was used to detect the signals.

2.10. Apoptosis assay

HaCaT at 1.0×10^5 cells/well, seeded in 12-well plates, were treated with Que. (30 or 90 μM/L) or DMSO. After 24 h, Hoechst 33342 staining assay and Flow cytometry were performed respectively. (1) Hoechst 33342 staining: the cells were stained with Hoechst 33342 (Beyotime Biotechnology, Shanghai, China) for 10 min and detection with the fluorescence microscopy (Olympus, Tokyo, Japan). (2) Flow cytometry analysis of apoptosis: the cells were stained for 15 min at room temperature in the dark with Annexin V-FITC/PI apoptosis kit (BD Biosciences), followed by the signals detection with flow cytometer (BD Biosciences).

2.11. RNA preparation, cDNA library establishment and RNAseq

Following extraction of RNAs using TRIzol reagent (Invitrogen, USA), RNA integrity number (RIN) value above 7.5 (evaluated by Agilent Bio-analyzer 2100) was identified as qualified for RNAseq. After removing the rRNAs, the mRNAs were fragmented for cDNAs amplification with random primers, followed by RNAseq using high-seq 4000 Illumina platform with a model of 2*150 bp.

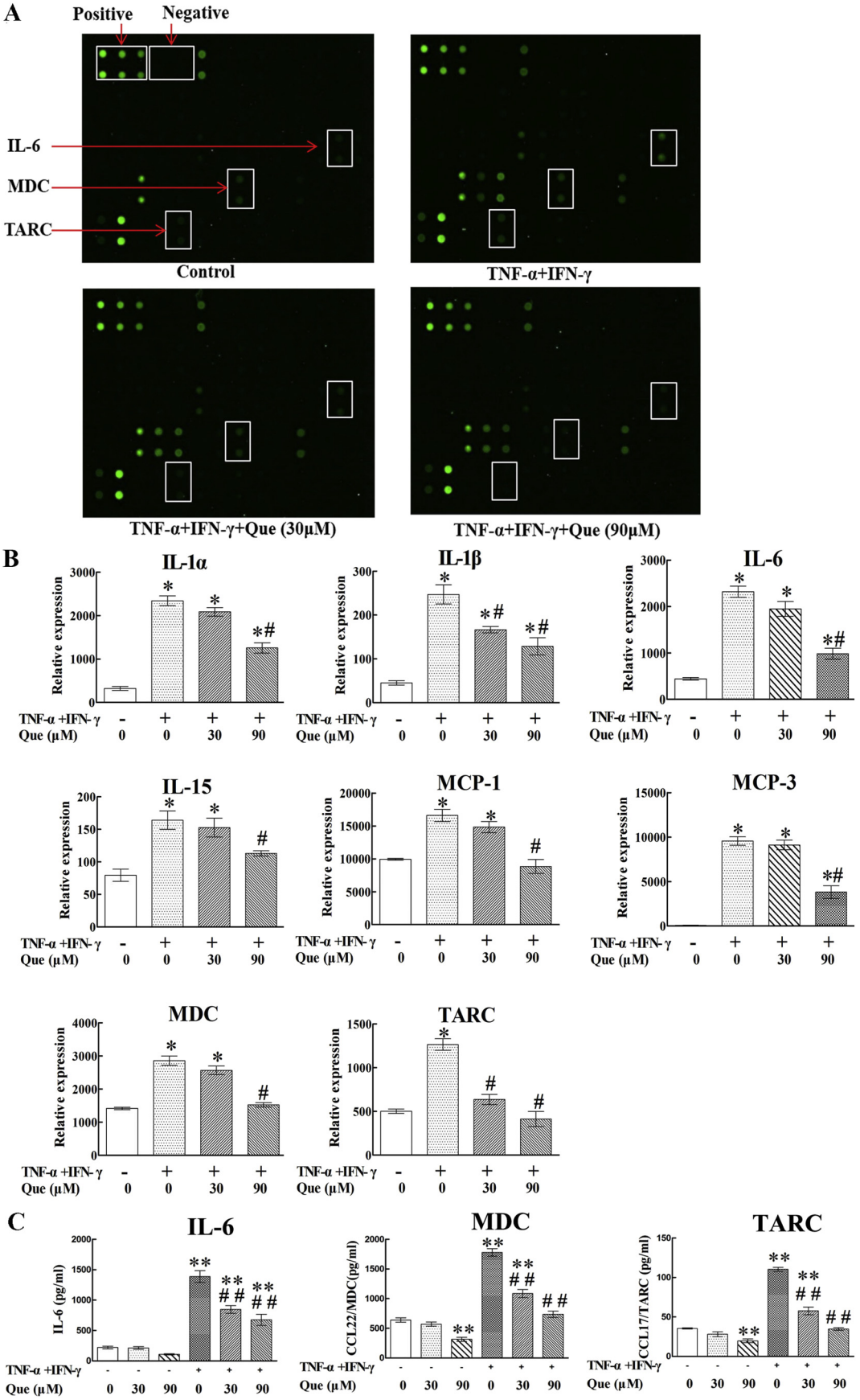

Fig. 3. Effects of quercetin (Que) on IFN-γ/TNF-α-induced chemokine expression profiling in HaCaT cells. Serum-free culture supernatants from HaCat cells of control, TNF-α + IFN-γ and TNF-α + IFN-γ + Que. group were analyzed by antibody arrays. A. The differentially expressed cytokines IL-6, MDC and TARC were marked in the microarray. B. The differentially expressed cytokines were all listed. Data are the means ± SEM (n = 3). C. Results of antibody arrays were verified by ELISA. Data are the means ± SEM (n = 5).*p < 0.05, * * p < 0.01 vs. the control group; # p < 0.05, ## p < 0.01 vs. the TNF-α/IFN-γ-treated group.

Table 2
Primers used for qRT-PCR.

lncRNA or mRNA	Primers
CXCL-5-forward	5-TGCTFCTTTGCCTACATTGCC -3
CXCL-5-reverse	5-GGAGCACTTGCCACTGGTGT −3
IL-6-forward	5-ACCTAGAGTACCTCCAGAACAGAT-3
IL-6-reverse	5-GCAGGAACTGGATCAGGACTTT −3
MCP-1-forward	5- CTAACCCAGAAACATCCAATTCTCA-3
MCP-1-reverse	5- AGCAGCAGGCACAGAAGG-3
RELA-forward	5- GAAGAAGAGTCCTTTCAGCG −3
RELA-reverse	5- GGGAGGACGTAAAGGGATAG −3
TLR-2-forward	5- CCCTTTTGCTTACTTCCTAGTCCCG-3
TLR-2-reverse	5- GAGGGAGGCATCTGGTAG-3
TLR-6-forward	5-AGTGGTGCCATTCGAACTCT −3
TLR-6-reverse	5-AGCCTTCAGCTTGTGGTACT −3
TNF-α-forward	5-CCTGCTGCACTTTGGAGTGA-3
TNF-α-reverse	5-GAGGGTTTGCTACAACATGGG-3
IL-1A-forward	5-AGATGCCTGAGATACCCAAAACC -3
IL-1A-reverse	5-CCAAGCACACCCAGTAGTCT-3
IL-1B-forward	5- TATTACAGTGGCAATGAGG −3
IL-1B-reverse	5- ATGAAGGGAAAGAAGGTG-3
HSPB1-forward	5- CAAGGATGGCGTGGTGGA-3
HSPB1-reverse	5- TCTCGTTGGACTGCGTGGC-3
MAP3K8-forward	5- AGCGCCAGGGCAGTGCTGGTCTGGG-3
MAP3K8-reverse	5- CCCAGACCAGCACTGCCCTGGCGCT-3
MAPKAPK-5-forward	5-GTCCCGGCGATGTGTGGCGCTGAGG-3
MAPKAPK-5-reverse	5-CCTCAGCGCCACACATCGCCGGGAC-3
lnc-C7orf30–2-forward	5- ATGGTGAATACCAAACTGGCC -3
lnc-C7orf30–2-reverse	5- CATGCAAGAAATGTGCCTGCT −3
lnc-C7orf30–3-forward	5- GATTGCCACTTGATGCCGC -3
lnc-C7orf30–3-reverse	5- TCCATGAGCCGAAAGCAAAG −3
lnc-B3GNT3–1-forward	5- CAGGGGTGAGGCGTGGGAGGGGTGC -3
lnc-B3GNT3–1-reverse	5- GCACCCCTCCCACGCCTCACCCCTG −3
lnc-C9orf68–3-forward	5- CCACAAGTGAATAAAGCTG −3
lnc-C9orf68–3-reverse	5- GGCTTCTTACATCATGGTTG −3
lnc-CCL2–8-forward	5- CCATCCAAGCAGACGTGGTA −3
lnc-CCL2–8-reverse	5- GGAGTAACTGCGCTGAGTGT −3
GAPDH-forward	5-AAGAGCACAAGAGGAAGAGAGAGAC-3
GAPDH-reverse	5-GTCTACATGGCAACTGTGAGGAG-3

Table 3
Target sequence of Smart Silencer.

Product ID	Target sequence of Smart Silencer
siG170823044825	ATACCAAACTGGCCTGTTA
siG170823044834	GCTACCAGATCTCAGTAAC
siG170823044840	GCATGAACAAGAGTAAATA
lnc6170823044910	AATGGTGAATACCAAACTGG
lnc6170823044925	CTAAAAGATGCTACCAGATC
lnc6170823044938	CCAGATCTCAGTAACTTTAC

2.12. Bioinformatics analysis

Differentially expressed genes obtained from RNAseq were performed GO terms and KEGG pathway analyses. For GO terms analysis, GO Seq R package was used and the GO terms showing $p < 0.05$ was seen as statistical significance. The website: http://www.genome.jp/kegg/ was used for KEGG analysis, followed by the statistical enrichment in KEGG pathways using the KOBAS software. Random Gene Set Enrichment Analysis (RGSEA) was performed for pathways enrichment assesee using random set of lncRNA in the genome.

2.13. Construction of differentially expressed lncRNAs/mRNAs co-expression network

For drawing network, we used critieria of $|COR| > 0.85$ and $P < 0.05$ to select the co-expressed lncRNAs and mRNAs. To map the network graphs interactd with lncRNAs' target genes, specific lncRNAs of the altered lncRNAs were selected, which could help the lncRNAs' holistic analysis in the samples.

2.14. qRT-PCR

For validation of the expression of significantly altered lncRNA and mRNA, qRT-PCR was performed. QIAzol (Qiagen, Valencia, CA, USA) was used for extracting the total RNA from each groups of the HaCat cells, followed by cDNA systenesis with (Promega). Then a 7300 Real-Time PCR System (Thermo, USA) was used to perform Real-time PCR. For relative quantification, $2^{-\Delta\Delta Ct}$ was calculated and used as an indication of gene relative expression. The PCR primers for amplifying the genes were listed in Table 2. The GAPDH gene was used as an internal control.

2.15. Inhibition of LncRNA

LncRNA Smart Silencer, is a mixture of three antisense oligonucleotides and three siRNAs (RiboBio, Guangzhou, China), was used for inhibiting the lncRNAs. The negative control Smart Silencer does not contain domains homologous to humans, mice and rats. The cultured HaCat cells supplemented with IFN-γ/TNF-α were divided into a lnc-C7orf30–2 (Table 3) Smart Silencer group, a negative control group, and a culture without IFN-γ/TNF-α termed as blank control group. For the transfection, Lipofectamine 2000 was used.

2.16. Statistical analysis

All data were processed using the SPSS 20.0 software (SPSS Inc., Chicago, IL, USA), which were expressed as mean ± SD. One-way ANOVA analysis was performed and $P < 0.05$ was defined as statistical significance. All the experiments were performed three times.

3. Results

3.1. Que suppressed MC903-induced AD skin lesions

We observed that in the MC903 group (Fig. 1A), left ears of the mice developed erythema and edema gradually, the average thickness increased significantly with dry and crusted phenotypes. After Que. application for 8 days, Que. obviously attenuated MC903-induced AD severity and the ear thickness. Compared to the AD model group, vehicle had no protective effect against AD-like skin lesions in mice (Fig. 1D and E).

Repetitive MC903 treatments induced epidermal thickness and hyperplasia, which was reversed by the application of Que. (Fig. 1B and F). Furthermore, Toluidine blue staining identified that MC903-increased mast cell numbers can be inhibited by Que. treatment (Fig. 1C and G).

3.2. Que suppressed inflammatory cytokines expressions in ear lesions of MC903-induced AD-like mice

As shown in Fig. 2, there were elevated IFN-γ, CCL17, CCL22, TNF-α, IL-4 and IL-6 levels in ear lesions of the AD model group compared with the normal control group. However, Que. application suppressed all of these inflammatory cytokines expressions.

3.3. Que altered the secretion of cytokines in IFN-γ/TNF-α-induced HaCat cells

We performed Cytokine Antibody Array assay which contained 120 cytokine proteins (Table 1), the results showed that Que. suppressed the level of IL-1α, IL-1β, IL-6, IL-15, MCP-1, MCP-3, CCL17 and CCL22 in the supernatants of the IFN-γ/TNF-α-treated HaCat cells (Fig. 3).

To corroborate the results of antibody arrays, IL-6, CCL17 and CCL22 was further detected using the ELISAs assay, the results showed that IL-6, CCL17 and CCL22 were decreased by Que. application in the IFN-γ/TNF-α-treated HaCat cells (Fig. 3C), which were consistent with

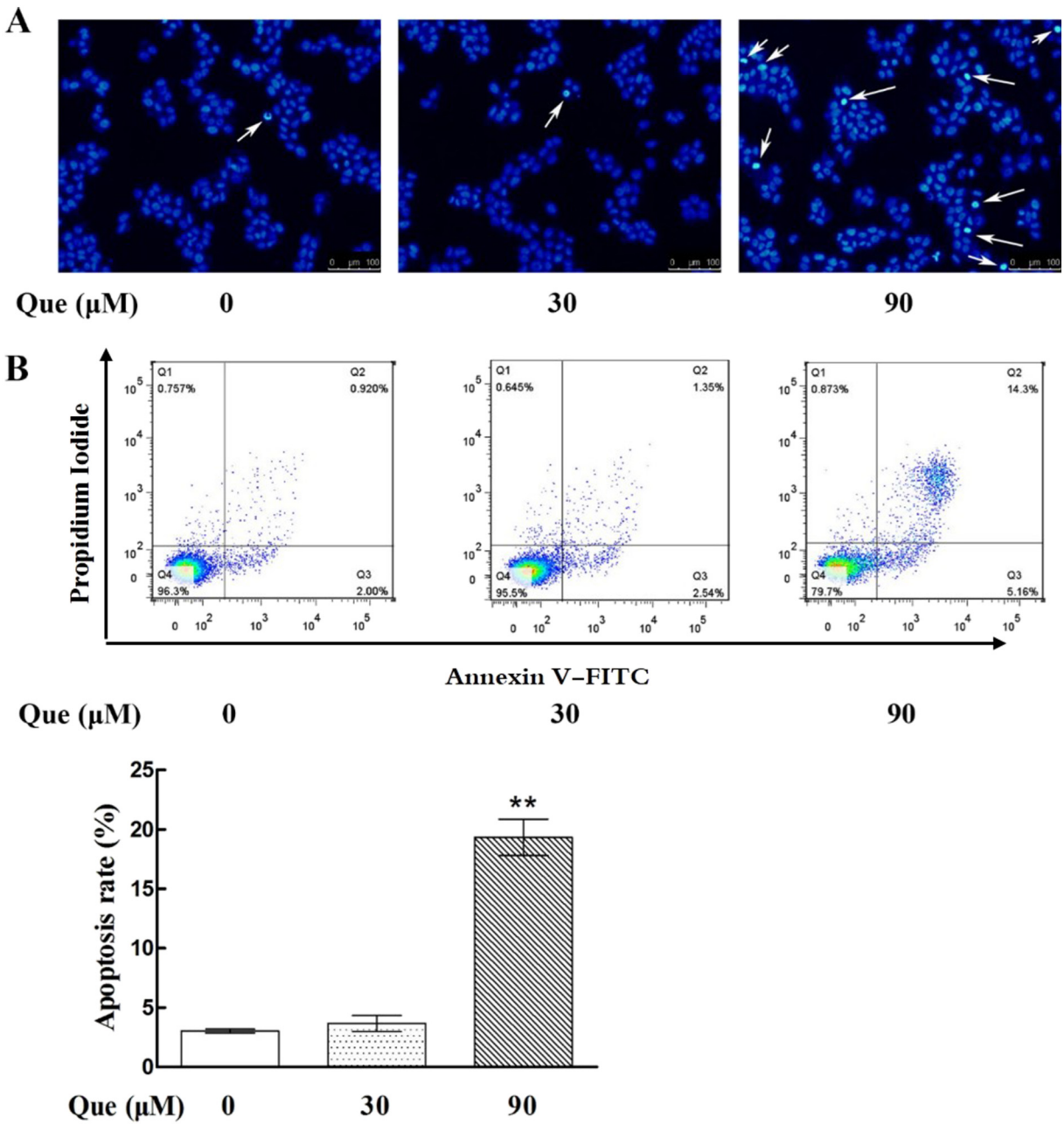

Fig. 4. Effects of Que. on apoptosis of HaCat cells. A. Hoechst 33342 staining showed that the apoptotic cells were round or oval-shaped, with bright-blue irregular nuclei ; B. Flow cytometry of Annexin V/PI-stained cells was used to quantify the apoptotic rate of the HaCat cells. **:$P < 0.01$, vs. the control group. (For interpretation of the references to colour in this figure legend, the reader is referred to the web version of this article.)

antibody array assay results, confirming the reliability of Cytokine Antibody Array assay. We detected the effects of Que. on HaCat cells without IFN-γ/TNF-α stimulation, results showed that 30 μM Que. had no significant effects on production of IL-6, MDC and TARC, 90 μM Que. could inhibit the production of both MDC and TARC ($P < 0.01$).

3.4. Effects of Que on apoptosis of HaCat cells

To examine whether Que. can affect the apoptosis of HaCat cells, we performed Annexin V-FITC/PI and hoechst 33342 staining assays, the results of two assays are consistent and showed that the 90 μM Que. treated HaCat cells had higher apoptotic rate compared with the control group ($P < 0.01$) (Fig. 4), while the 30 μM Que. had no obvious effect ($P > 0.05$).

3.5. LncRNAs and mRNAs expression profile in Que-treated HaCaT cells induced by IFN-γ/TNF-α

To profile the expressions of lncRNA and mRNA, high-throughput sequencing was performed, followed by screening by volcano plot using the criteria log2 (fold change) > 1; $q < 0.05$, and the coding and non-coding genes with expression differentially were screened (Fig. 5A and C). We observed that a total of 1141 lncRNAs were upregulated, while 825 were downregulated. For mRNA transcripts, 969 exhibited upregulation and 784 exhibited downregulation in IFN-γ/TNF-α-induced HaCat cells and control cells. In Que. treated and non-treated HaCat cells induced by IFN-γ/TNF-α, a total of 278 lncRNAs upregulation and 254 downregulation, and a total of 144 mRNA transcripts upregulation and 147 downregulation were observed (Fig. 5B and D).

We further performed GO terms and KEGG pathway analysis to

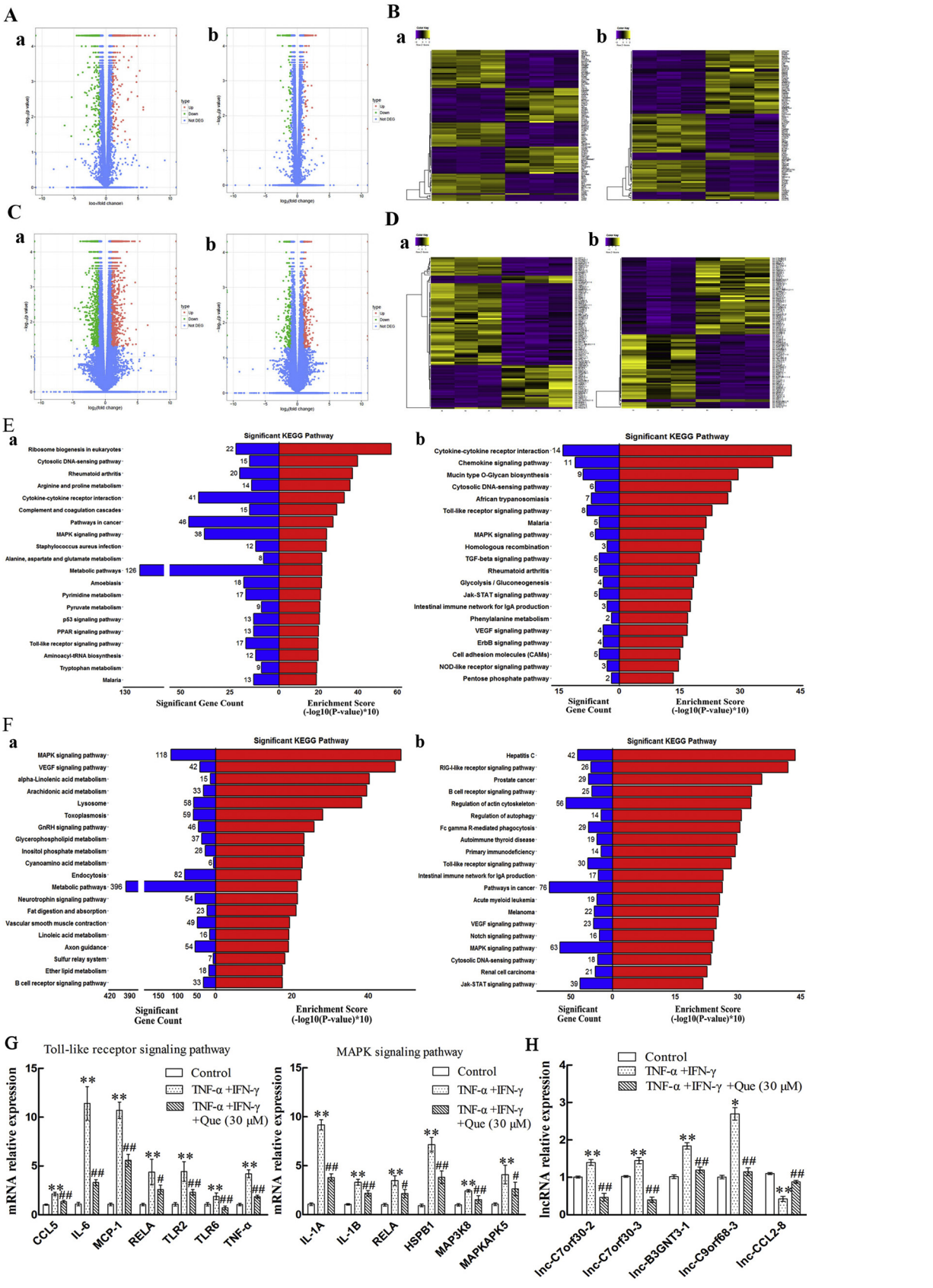

(caption on next page)

Fig. 5. Differentially expressed lncRNAs and mRNAs. A. The volcano plot illustrates the differentially expressed mRNAs. B. The hierarchical cluster analysis generated heat maps of the top 100 significant differential expressed mRNAs. C. The volcano plot illustrates the differentially expressed lncRNAs. D. The hierarchical cluster analysis generated heat maps of the top 100 significant differential expressed lncRNAs. E. The top 20 KEGG pathways of significantly differentially expressed mRNAs. F. The top 20 KEGG pathways of significantly differentially expressed lncRNAs. G. qRT-PCR validation of differential expressions of mRNAs involved in Toll-like receptor signaling pathway and MAPK signaling pathway. H. qRT-PCR validation of differential expression levels of lncRNAs. a. TNF-α + IFN-γ Vs Control b. TNF-α + IFN-γ + Que. Vs TNF-α + IFN-γ. **P < 0.01, TNF-α + IFN-γ Vs Control. ## P < 0.01, TNF-α + IFN-γ + Que. Vs TNF-α + IFN-γ, # P < 0.05, TNF-α + IFN-γ + Que. Vs TNF-α + IFN-γ.

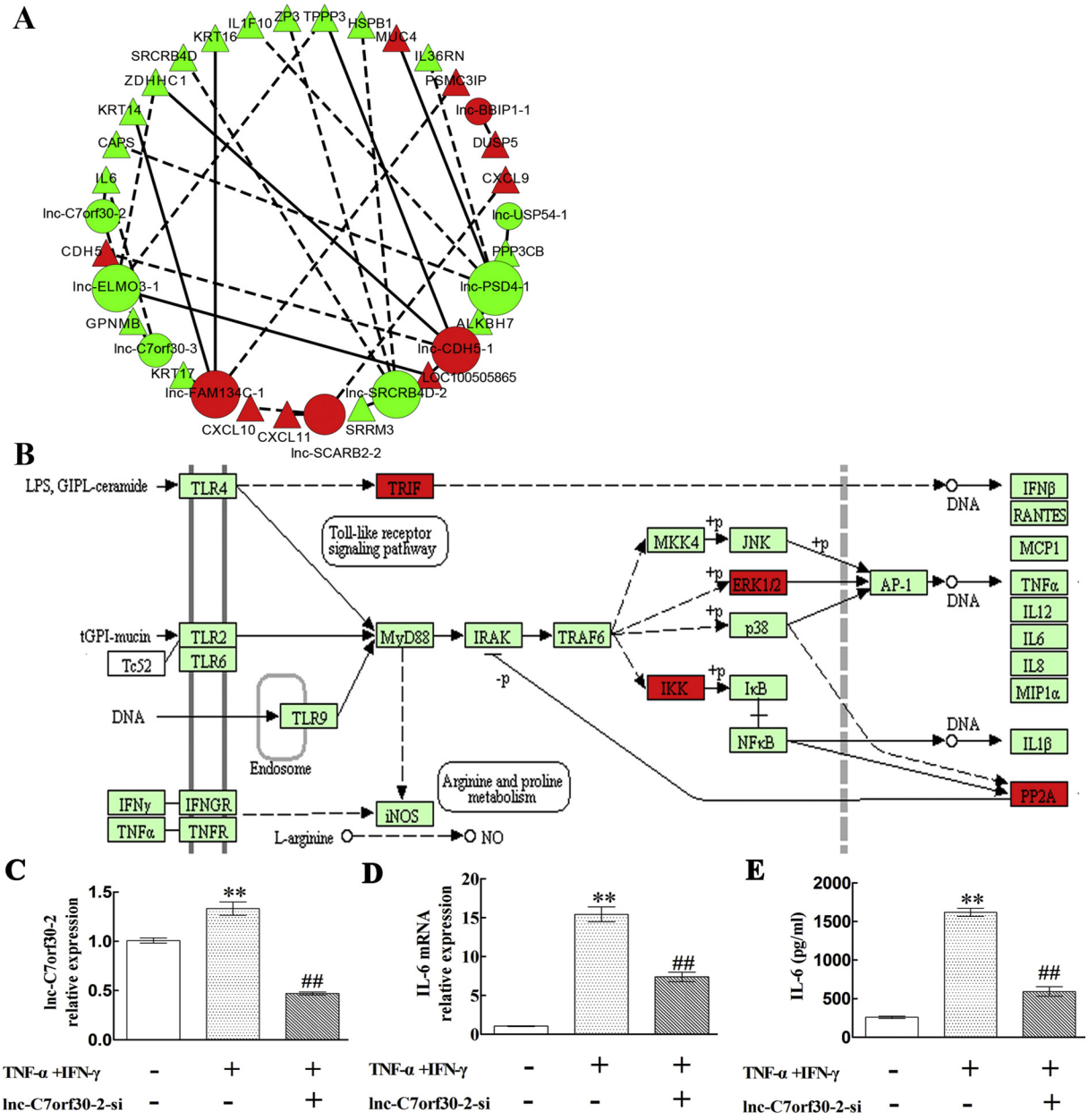

Fig. 6. LncRNA/mRNA transcripts co-expression network in quercetin-treated HaCaT cells induced by IFN-γ/TNF-α. (A) The network represents the co-expression correlations between the significantly differentially expressed mRNA and lncRNA transcripts (|COR| > 0.95, $P < 0.05$). Circles indicate lncRNA transcripts and triangles indicate mRNA transcripts. Solid lines indicate positive correlations, and dashed lines indicate negative correlations. Red represents upregulated, and green represents downregulated. (B) KEGG analysis suggested that lncRNA-coexpressed mRNAs were mainly targeted to the Toll-like receptor signaling pathway. C, D and E. Effect of lnc-C7orf30–2 RiboTM lncRNA Smart Silencer on expression of IL-6 in TNF-α/IFN-γ induced HaCaT cells. C. lnc-C7orf30–2 ; D. IL-6 mRNA; E.IL-6. ** p < 0.01, vs. the control group ; ## p < 0.01, vs. TNF-α/IFN-γ induced HaCaT cells. (For interpretation of the references to colour in this figure legend, the reader is referred to the web version of this article.)

construct mRNA and lncRNAs regulation pathways, which indicated their relationship with inflammation, including signaling pathways of cytokine-cytokine receptor interaction, toll-like receptor and MAPK (Fig. 5E and F). We then validated differentially expressed mRNAs and lncRNAs with qRT-PCR, which verified the accuracy of high-throughput sequencing analysis (Fig. 5G and H).

3.6. Co-expression networks of lncRNA/mRNA transcripts

To reveal the potential mechanisms of Que. mediated anti-inflammatory effects, we constructed a co-expression network of lncRNA/mRNA, which showed that the correlation of lnc-C7orf30–2 and IL-6 mRNA transcripts had the highest COR-value (COR: 0.999, $P < 0.05$) in the regulation of the toll-like receptor signaling pathway (Fig. 6A and B).

We further studied the effect of lnc-C7orf30–2 knockdown on the expression of IL-6. Lnc-C7orf30–2 Smart Silencer were transfected into IFN-γ/TNF-α-induced HaCaT cells, which showed that the level of lnc-C7orf30–2 was markedly reduced by > 50% ($P < 0.01$) (Fig. 6C), while the IL-6 mRNA and protein expressions were both sharply increased ($P < 0.01$) (Fig. 6D and E).

4. Discussion

In the present study, we identified the regulatory mechanisms of Que.'s inhibitory effects on MC903-induced AD mouse model. Results showed that Que. markedly suppressed the AD severity, and the ear epidermis thickness. These data demonstrated that Que. exhibited protective function of MC903-induced AD mouse model.

AD symptoms is characterized by mast cells infiltration, leading to the release of allergic mediators [17]. Mast cells are widely recognized as crucial factor responsible for allergic inflammatory reactions. Studies demonstrated that high IgE levels activate mast cells. The IgE receptor FcεRI sits on the cell surface of mast cells, as effector cells, release histamines and other biologically active products that trigger allergic inflammatory symptoms [18]. Therefore, methods that reduce the number of mast cells and inhibit their activation may ameliorate the symptoms of AD [19]. Histologically, our results confirmed the ear skin tissue of MC903-sensitized mice had high level infiltration of inflammatory cells, while Que. application can reduce the inflammatory cells and mast cells infiltration.

Keratinocytes, the major cell types of epidermis, mediated the pathogenesis of inflammatory skin diseases [20]. They can secret proinflammatory cytokines and chemokines in external environment alterations, such as UV light, microbiological agents and allergens [21,22]. The treatment of keratinocytes with TNF-α and IFN-γ can result alterations of cytokines and chemokines, while downregulation of which can exert an protective effect for the inflammatory skin diseases [23,24]. Here, we investigated the anti-inflammatory effects of Que. both in vivo and in vitro. Results showed that MC903 induced up-regulation of CCL17, CCL22, IL-4, IL-6, IFN-γ and TNF-α expression in skin lesions of AD-like mouse model, while Que. application suppressed all of these inflammatory cytokines expressions.

Alterations of Th2/Th1 cytokines secretion were considered as a pathological factor of AD [25]. It has been confirmed that in the patients with atopic dermatitis, the levels of CCL17 and CCL22 in the serum were markedly increased [26]. CCR4, the receptor of CCL17 and CCL22, is predominantly expressed on Th2 lymphocytes and regulates the migration of Th2 lymphocytes into the site of inflammation [27]. Therefore, CCL17 and CCL22 are considered pivotal in the development of Th2-dominant inflammatory skin diseases, including AD [28]. IL-4 cound induce B-cell class switch to IgE, and serve as a diffenetiation factor for Th2 cells [29]. IL-4 elevation in AD skin lesion can lead to allergic inflammation, resulting in intraepidermal and pruritus edema [29,30]. IFN-γ, a key Th1 effector cytokine, was also up-regulated in chronic AD-like skin lesions of mice [31]. Up-regulation of IFN-γ can decrease the ceramides with long chain fatty acids, contributing to the abnormality of the permeability barrier function [32]. In this study, Que. suppressed the levels of CCL17, CCL22, IL-4, IFN-γ in AD like skin, demonstrating that the anti-inflammatory function of Que.

To profile the effect of Que. on cytokines released from HaCat cells treated with IFN-γ/TNF-α, Cytokine Antibody Arrays were used and the results showed that 30 μM and 90 μM Que. could both inhibit the level of proinflammatory cytokines IL-1α, IL-1β, IL-6, IL-15, as well as MCP-1, MCP-3, CCL17 and CCL22 [33–36]. IL-6, a cytokine secreted by keratinocytes, is involved in many inflammatory skin diseases, including psoriasis and AD [34]. A large number of inflammatory stimuli can induce the expression of IL-6 [33,37]. Both IL-1α and IL-1β can stimulate cytokine production [37,38]. IL-15 can induce TNF-α and IL-17 production, neutrophil and macrophage recruitment [39,40]. MCP-1 and MCP-3 are chemokines, which can attract several types of leukocytes [41]. The results of Cytokine Antibody Arrays were validated by ELISA. Results of validation confirmed the reliability and validity of Cytokine Antibody Arrays. We detected the effects of Que. on HaCat cells without IFN-γ/TNF-α stimulation, results showed that 30 μM Que. had no significant effects on production of IL-6, MDC and TARC, 90 μM Que. could inhibit the production of both MDC and TARC. The inhibition of the production of MDC and TARC of 90 μM may be relation to the effects of promoting apoptosis. We selected 30 μM as the concentration used in subsequent experiments.

Dysregulated lncRNA and mRNAs, identified using RNA sequencing in HaCat cells treated with IFN-γ/TNF-α before and after treated by Que., were then analyzed by KEGG and GO terms, which showed the significant differential expressed mRNAs and lncRNA were associated with inflammation related pathways including signaling pathways of JAK-STAT, toll-like receptor, MAPK and chemokine.

Toll-like Receptors (TLRs) signaling pathway can trigger innate immune response, leading the inflammation in higher animals [42]. In human skin, TLRs are expressed in keratinocytes [43,44]. Study have suggested that TLR2 is associated with the pathogenesis of AD [45]. The expression of TLR2 is correlated with the levels of IL-6 [46,47]. In our study, the results showed that cells treated with IFN-γ/TNF-α could up-regulate the mRNA expressions of TLR2, TLR6, CCL5, IL-6, MCP-1, RELA and TNF-α in HaCat cells, Que. could down-regulate all these mRNAs expressions in HaCat cells treated with IFN-γ/TNF-α, suggesting that Que. may inhibit the level of CCL5, IL-6, MCP-1, RELA and TNF-α through the TLR2 and TLR6 signaling pathway.

In particular, the co-expression network was performed to explore the potential mechanism of lncRNAs, which indicated that lnc-C7orf30–2 was highly correlated with IL-6. In vitro study suggested that Lnc-C7orf30–2 knockdown can decrease the IL-6 mRNA and protein expressions.

In summary, the data here showed that topical application of Que. can exert beneficial effects in MC903-induced AD like lesions. Results of in vitro demonstrates that Que. could inhibit proinflammatory chemokines and cytokines in IFN-γ/TNF-α-treated HaCat cells. Furthermore, high-throughput sequencing showed that the mRNAs and LncRNAs were significantly differentially expressed after Que. treatment. The co-expression network indicated that lnc-C7orf30–2 and IL-6 were highly correlated. Knockdown of lnc-C7orf30–2 reduced IL-6 mRNA and protein expression. These data demonstrated that lnc-C7orf30–2 may mediate the anti-inflammatory effect of Que., which might be a useful target for the AD treatment.

Declaration of Competing Interest

The authors state no conflict of interest.

Acknowledgment

This project was supported by the National Natural Science Foundation of China (81774023), the China Postdoctoral Science Foundation (2015M571345), and Liaoning Research and Development Directory project and 111 project (D18011).

References

[1] L. Bin, D.Y. Leung, Genetic and epigenetic studies of atopic dermatitis, Allergy, Asthma Clin. Immunol. 12 (2016) 52.

[2] M.C. Zaniboni, L.P. Samorano, R.L. Orfali, V. Aoki, Skin barrier in atopic dermatitis: beyond filaggrin, An. Bras. Dermatol. 91 (4) (2016) 472–478.
[3] S. Caglayan Sozmen, M. Karaman, S. Cilaker Micili, S. Isik, Z. Arikan Ayyildiz, A. Bagriyanik, N. Uzuner, O. Karaman, Resveratrol ameliorates 2,4-dinitrofluorobenzene-induced atopic dermatitis-like lesions through effects on the epithelium, PeerJ 4 (2016) e1889.
[4] W.D. Boothe, J.A. Tarbox, M.B. Tarbox, Atopic dermatitis: pathophysiology, Adv. Exp. Med. Biol. 1027 (2017) 21–37.
[5] K.F. Huang, K.H. Ma, P.S. Liu, B.W. Chen, S.H. Chueh, Baicalein increases keratin 1 and 10 expression in HaCaT keratinocytes via TRPV4 receptor activation, Exp. Dermatol. 25 (8) (2016) 623–629.
[6] Y.Y. Sung, Y.S. Kim, H.K. Kim, Illicium verum extract inhibits TNF-alpha- and IFN-gamma-induced expression of chemokines and cytokines in human keratinocytes, J. Ethnopharmacol. 144 (1) (2012) 182–189.
[7] T. Kanazawa, Y. Shizawa, M. Takeuchi, K. Tamano, H. Ibaraki, Y. Seta, Y. Takashima, H. Okada, Topical anti-nuclear factor-kappa B small interfering RNA with functional peptides containing sericin-based hydrogel for atopic dermatitis, Pharmaceutics 7 (3) (2015) 294–304.
[8] Z. Hussain, H. Katas, M.C. Mohd Amin, E. Kumolosasi, S. Sahudin, Downregulation of immunological mediators in 2,4-dinitrofluorobenzene-induced atopic dermatitis-like skin lesions by hydrocortisone-loaded chitosan nanoparticles, Int. J. Nanomedicine 9 (2014) 5143–5156.
[9] M. Osada-Oka, S. Hirai, Y. Izumi, K. Misumi, K. Samukawa, S. Tomita, K. Miura, Y. Minamiyama, H. Iwao, Red ginseng extracts attenuate skin inflammation in atopic dermatitis through p70 ribosomal protein S6 kinase activation, J. Pharmacol. Sci. 136 (1) (2018) 9–15.
[10] R.C. Barcelos, C. de Mello-Sampayo, C.T. Antoniazzi, H.J. Segat, H. Silva, J.C. Veit, J. Piccolo, T. Emanuelli, M.E. Burger, B. Silva-Lima, L.M. Rodrigues, Oral supplementation with fish oil reduces dryness and pruritus in the acetone-induced dry skin rat model, J. Dermatol. Sci. 79 (3) (2015) 298–304.
[11] S.J. Jeon, M.O. Kim, F. Ali-Shah, P.O. Koh, Quercetin attenuates the injury-induced reduction of gamma-enolase expression in a middle cerebral artery occlusion animal model, Lab. Anim. Res. 33 (4) (2017) 308–314.
[12] M. Ahmad, M. Sultana, R. Raina, N.K. Pankaj, P.K. Verma, S. Prawez, Hypoglycemic, hypolipidemic, and wound healing potential of quercetin in streptozotocin-induced diabetic rats, Pharmacogn. Mag. 13 (Suppl. 3) (2017) S633–s639.
[13] L. Zhao, F. Cen, F. Tian, M.J. Li, Q. Zhang, H.Y. Shen, X.C. Shen, M.M. Zhou, J. Du, Combination treatment with quercetin and resveratrol attenuates high fat diet-induced obesity and associated inflammation in rats via the AMPKalpha1/SIRT1 signaling pathway, Exp. Ther. Med. 14 (6) (2017) 5942–5948.
[14] J. Dai, M.K. Choo, J.M. Park, D.E. Fisher, Topical ROR inverse agonists suppress inflammation in mouse models of atopic dermatitis and acute irritant dermatitis, J. Invest. Dermatol. 137 (12) (2017) 2523–2531.
[15] X.J. Liu, Z.L. Mu, Y. Zhao, J.Z. Zhang, Topical tetracycline improves MC903-induced atopic dermatitis in mice through inhibition of inflammatory cytokines and thymic stromal lymphopoietin expression, Chin. Med. J. 129 (12) (2016) 1483–1490.
[16] J.H. Choi, S.W. Jin, B.H. Park, H.G. Kim, T. Khanal, H.J. Han, Y.P. Hwang, J.M. Choi, Y.C. Chung, S.K. Hwang, T.C. Jeong, H.G. Jeong, Cultivated ginseng inhibits 2,4-dinitrochlorobenzene-induced atopic dermatitis-like skin lesions in NC/Nga mice and TNF-alpha/IFN-gamma-induced TARC activation in HaCaT cells, Food Chem. Toxicol. 56 (2013) 195–203.
[17] D.D. Hou, Z.H. Di, R.Q. Qi, H.X. Wang, S. Zheng, Y.X. Hong, H. Guo, H.D. Chen, X.H. Gao, Sea buckthorn (Hippophae rhamnoides L.) oil improves atopic dermatitis-like skin lesions via inhibition of NF-kappaB and STAT1 activation, Skin Pharmacol. Physiol. 30 (5) (2017) 268–276.
[18] K. Malik, K.D. Heitmiller, T. Czarnowicki, An update on the pathophysiology of atopic dermatitis, Dermatol. Clin. 35 (3) (2017) 317–326.
[19] Y. Meng, Z. Liu, C. Zhai, T. Di, L. Zhang, L. Zhang, X. Xie, Y. Lin, N. Wang, J. Zhao, Y. Wang, P. Li, Paeonol inhibits the development of 1chloro2,4dinitrobenzeneinduced atopic dermatitis via mast and T cells in BALB/c mice, Mol. Med. Rep. 19 (4) (2019) 3217–3229.
[20] J.Y. Kee, Y.D. Jeon, D.S. Kim, Y.H. Han, J. Park, D.H. Youn, S.J. Kim, K.S. Ahn, J.Y. Um, S.H. Hong, Korean red ginseng improves atopic dermatitis-like skin lesions by suppressing expression of proinflammatory cytokines and chemokines in vivo and in vitro, J. Ginseng Res. 41 (2) (2017) 134–143.
[21] H. Uchi, H. Terao, T. Koga, M. Furue, Cytokines and chemokines in the epidermis, J. Dermatol. Sci. 24 (Suppl. 1) (2000) S29–S38.
[22] H.J. Jeong, H.Y. Kim, H.M. Kim, Molecular mechanisms of anti-inflammatory effect of chrysophanol, an active component of AST2017-01 on atopic dermatitis in vitro models, Int. Immunopharmacol. 54 (2018) 238–244.
[23] J.H. Yang, J.M. Yoo, E. Lee, B. Lee, W.K. Cho, K.I. Park, J. Yeul Ma, Anti-inflammatory effects of Perillae Herba ethanolic extract against TNF-alpha/IFN-gamma-stimulated human keratinocyte HaCaT cells, J. Ethnopharmacol. 211 (2018) 217–223.
[24] E.H. Han, Y.P. Hwang, J.H. Choi, J.H. Yang, J.K. Seo, Y.C. Chung, H.G. Jeong, Psidium guajava extract inhibits thymus and activation-regulated chemokine (TARC/CCL17) production in human keratinocytes by inducing heme oxygenase-1 and blocking NF-kappaB and STAT1 activation, Environ. Toxicol. Pharmacol. 32 (2) (2011) 136–145.
[25] Y.Y. Choi, M.H. Kim, H. Lee, S.Y. Jo, W.M. Yang, (R)-(+)-pulegone suppresses allergic and inflammation responses on 2,4-dinitrochlorobenzene-induced atopic dermatitis in mice model, J. Dermatol. Sci. 91 (3) (2018) 292–300.
[26] Y. Shimada, K. Takehara, S. Sato, Both Th2 and Th1 chemokines (TARC/CCL17, MDC/CCL22, and Mig/CXCL9) are elevated in sera from patients with atopic dermatitis, J. Dermatol. Sci. 34 (3) (2004) 201–208.
[27] G.A. Mostafa, H.Y. Tomoum, S.A. Salem, M.M. Abd El-Aziz, D.I. Abou El-Maged, I. El-Sayed El-Far, Serum concentrations of CCR4 ligands in relation to clinical severity of atopic dermatitis in Egyptian children, Pediatr. Allergy Immunol. 19 (8) (2008) 756–762.
[28] S.M. Ju, H.Y. Song, S.J. Lee, W.Y. Seo, D.H. Sin, A.R. Goh, Y.H. Kang, I.J. Kang, M.H. Won, J.S. Yi, D.J. Kwon, Y.S. Bae, S.Y. Choi, J. Park, Suppression of thymus- and activation-regulated chemokine (TARC/CCL17) production by 1,2,3,4,6-penta-O-galloyl-beta-D-glucose via blockade of NF-kappaB and STAT1 activation in the HaCaT cells, Biochem. Biophys. Res. Commun. 387 (1) (2009) 115–120.
[29] S.R. Kim, H.S. Choi, H.S. Seo, J.M. Ku, S.H. Hong, H.H. Yoo, Oral Administration of Herbal Mixture Extract Inhibits 2,4-Dinitrochlorobenzene-Induced Atopic Dermatitis in BALB/c Mice, 2014 (2014), p. 319438.
[30] J.G. Park, Y.S. Yi, Tabetri (Tabebuia Avellanedae Ethanol Extract) Ameliorates Atopic Dermatitis Symptoms in Mice, 2018 (2018), p. 9079527.
[31] D.Y. Leung, N. Jain, H.L. Leo, New concepts in the pathogenesis of atopic dermatitis, Curr. Opin. Immunol. 15 (6) (2003) 634–638.
[32] K.R. Feingold, The adverse effect of IFN gamma on stratum corneum structure and function in psoriasis and atopic dermatitis, J. Invest. Dermatol. 134 (3) (2014) 597–600.
[33] T. Kishimoto, Interleukin-6: from basic science to medicine–40 years in immunology, Annu. Rev. Immunol. 23 (2005) 1–21.
[34] N.A. Razali, N.A. Nazarudin, K.S. Lai, F. Abas, S. Ahmad, Curcumin derivative, 2,6-bis(2-fluorobenzylidene)cyclohexanone (MS65) inhibits interleukin-6 production through suppression of NF-kappaB and MAPK pathways in histamine-induced human keratinocytes cell (HaCaT), BMC Complement. Altern. Med. 18 (1) (2018) 217.
[35] A. Lesiak, I. Bednarski, M. Palczynska, E. Kumiszcza, M. Kraska-Gacka, A. Wozniacka, J. Narbutt, Are interleukin-15 and -22 a new pathogenic factor in pustular palmoplantar psoriasis? Postepy dermatologii i alergologii 33 (5) (2016) 336–339.
[36] W.K. Ko, S.H. Lee, S.J. Kim, M.J. Jo, H. Kumar, I.B. Han, S. Sohn, Anti-inflammatory effects of ursodeoxycholic acid by lipopolysaccharide-stimulated inflammatory responses in RAW 264.7 macrophages, PLoS One 12 (6) (2017) e0180673.
[37] M. Hayashi, J. Takai, L. Yu, H. Motohashi, T. Moriguchi, M. Yamamoto, Whole-body in vivo monitoring of inflammatory diseases exploiting human interleukin 6-luciferase transgenic mice, Mol. Cell. Biol. 35 (20) (2015) 3590–3601.
[38] R. Asahina, S. Maeda, A review of the roles of keratinocyte-derived cytokines and chemokines in the pathogenesis of atopic dermatitis in humans and dogs, Vet. Dermatol. 28 (1) (2017) 16–e5.
[39] M.O. Danso, V. van Drongelen, A. Mulder, J. van Esch, H. Scott, J. van Smeden, A. El Ghalbzouri, J.A. Bouwstra, TNF-alpha and Th2 cytokines induce atopic dermatitis-like features on epidermal differentiation proteins and stratum corneum lipids in human skin equivalents, J. Invest. Dermatol. 134 (7) (2014) 1941–1950.
[40] A. Michalak-Stoma, A. Pietrzak, J.C. Szepietowski, A. Zalewska-Janowska, T. Paszkowski, G. Chodorowska, Cytokine network in psoriasis revisited, Eur. Cytokine Netw. 22 (4) (2011) 160–168.
[41] W.L. Thompson, L.J. Van Eldik, Inflammatory cytokines stimulate the chemokines CCL2/MCP-1 and CCL7/MCP-3 through NFkB and MAPK dependent pathways in rat astrocytes [corrected], Brain Res. 1287 (2009) 47–57.
[42] N.N. Kuzmich, K.V. Sivak, V.N. Chubarev, Y.B. Porozov, T.N. Savateeva-Lyubimova, F. Peri, TLR4 signaling pathway modulators as potential therapeutics in inflammation and sepsis, Vaccines 5 (4) (2017).
[43] S.S. Kang, L.S. Kauls, A.A. Gaspari, Toll-like receptors: applications to dermatologic disease, J. Am. Acad. Dermatol. 54 (6) (2006) 951–83; quiz 983-6.
[44] N.N. Tsybikov, I. Petrisheva, E.V. Fefelova, B.I. Kuznik, E. Magen, Expression of TLR2 and TLR4 on peripheral blood monocytes during exacerbation of atopic dermatitis, Allergy Asthma Proc. 36 (6) (2015) e140–e145.
[45] I.H. Kuo, A. Carpenter-Mendini, T. Yoshida, L.Y. McGirt, A.I. Ivanov, K.C. Barnes, R.L. Gallo, A.W. Borkowski, K. Yamasaki, D.Y. Leung, S.N. Georas, A. De Benedetto, L.A. Beck, Activation of epidermal toll-like receptor 2 enhances tight junction function: implications for atopic dermatitis and skin barrier repair, J. Invest. Dermatol. 133 (4) (2013) 988–998.
[46] F. Sanchez-Munoz, G. Fonseca-Camarillo, M.A. Villeda-Ramirez, E. Miranda-Perez, E.J. Mendivil, R. Barreto-Zuniga, M. Uribe, R. Bojalil, A. Dominguez-Lopez, J.K. Yamamoto-Furusho, Transcript levels of toll-like receptors 5, 8 and 9 correlate with inflammatory activity in ulcerative colitis, BMC Gastroenterol. 11 (2011) 138.
[47] N. Kordjazy, A. Haj-Mirzaian, A. Haj-Mirzaian, M.M. Rohani, E.W. Gelfand, N. Rezaei, A.H. Abdolghaffari, Role of toll-like receptors in inflammatory bowel disease, Pharmacol. Res. 129 (2018) 204–215.